

## Supporting Information

### Counting DNA Molecules with Visual Segments-based Readouts in Minutes

Rui Wang<sup>a+</sup>, Fang Zhang<sup>b+</sup>, Cheng Qian<sup>a</sup>, Cui Wu<sup>a</sup>, Zunzhong Ye<sup>a</sup>, Liu Wang<sup>a</sup>, Wenjuan Qian<sup>a</sup>, Jianfeng Ping<sup>a</sup>, Jian Wu<sup>a\*</sup>, and Yibin Ying<sup>a,c</sup>

**Abstract:** An ultrafast and extremely simple approach was proposed to count the number of DNA molecules in large reaction volume (~microliters), without any pre-modification or physical separation process. This method was generally based on the ultrafast property of PCR in capillary and extremely weak convection and diffusion effect of amplicon molecules in the thin flexible plastic tube. Rapid PCR was conducted in a plastic capillary tube. After amplification, every DNA molecule would generate a fluorescent amplicon cluster with the size of around 3 mm, forming visible discrete segments in the reaction plastic tube. By directly counting the number of amplicon cluster segments, the absolute amount of DNA molecules could be known. In this way, with a very simple home-made device, DNA counting at the level of single molecule can be successfully realized.

---

## Table of Contents

<b>Amplicon cluster diffusion process</b> .....	(Flash in ESI)
<b>Auto rapid PCR amplification process</b> .....	(Video in ESI)
<b>Experimental Procedures</b> .....	3
Materials and reagents.....	3
Heat transfer modeling analysis.....	3
Mock rapid PCR and real-time temperature measurement.....	3
DNA extraction and template preparation.....	3
DNA copies theoretical calculation.....	3
Amplicon counting process with modified rapid PCR.....	4
Gel electrophoresis imaging.....	4
<b>Results and Discussion</b> .....	5
<b>Heat transfer modeling analysis</b> .....	5
<b>Table S1</b> Thermo property of materials .....	6
<b>Figure S1</b> Numerical simulation condition.....	7
<b>Figure S2</b> Numerical and 2D simulation results for plastic tube and inside water.....	8
<b>Figure S3</b> Numerical and 2D simulation results for plastic tube and inside water.....	9
<b>Mock rapid PCR</b> .....	10
<b>Figure S4</b> The home-made device for rapid PCR amplification.....	11
<b>Figure S5</b> Thermal trace vs. time during rapid PCR amplification.....	12
<b>Investigation of rapid PCR amplification</b> .....	13
<b>Table S2</b> The targets, primer sequences and product sizes of rapid and traditional PCR.....	14
<b>Table S3</b> Reaction conditions of rapid and traditional PCR .....	15
<b>Figure S6</b> Rapid PCR amplification with Taq™ polymerase.....	16
<b>Figure S7</b> Rapid PCR amplification with SpeedSTAR™ polymerase.....	17
<b>Figure S8</b> Rapid PCR amplification with MightyAmp™ Ver.3 polymerase.....	18
<b>Figure S9</b> Rapid PCR amplification with Ex Taq™ polymerase.....	19
<b>Figure S10</b> Rapid PCR amplification with Z-Taq™ polymerase.....	20
<b>Figure S11</b> Selectivity of rapid PCR amplification for T- <i>nos</i> gene detection.....	21
<b>Figure S12</b> Sequencing and blast results of rapid PCR amplicon.....	22
<b>DNA molecules counting with rapid PCR</b> .....	24
<b>Figure S13</b> The excluded samples for DNA molecules counting.....	25
<b>Figure S14</b> The images of samples with different template concentrations.....	26
<b>Figure S15</b> The amplicon cluster diffusion process under room temperature.....	27
<b>Figure S16</b> The images of amplicon cluster for 50 samples.....	28
<b>DNA molecules detection and counting with 3 other kinds of genomic DNA</b> .....	29
<b>Figure S17-S18</b> <i>CaMV35S</i> gene detection and counting with rapid PCR amplification.....	29
<b>Figure S19-S21</b> <i>tlh</i> gene detection and counting with rapid PCR amplification.....	31
<b>Figure S22-S24</b> <i>IHHNV</i> gene detection and counting with rapid PCR amplification.....	34
<b>Figure S25</b> Traditional PCR amplification for 50 samples detection.....	37
<b>References</b> .....	37

---

## Experimental Procedures

### Materials and reagents

The flexible polypropylene (pp) plastic tube with 0.4 mm of inner diameter was purchased from Yongfa Plastic Co., Ltd. (Shanghai, China). Agarose was purchased from Sinopharm Chemical Reagent Co., Ltd. (Shanghai, China). All primers were synthesized by Sangon Biotechnology Co., Ltd. (Shanghai, China). The DNA amplicon were sequenced by BioSune Biotechnology Co., Ltd. (Hangzhou, China). TIANamp Plant/Bacteria/Virus DNA kits were purchased from Tiangen Biotechnology Co., Ltd. (Beijing, China). Taq™ polymerase, SpeedSTAR™ polymerase, MightyAmp™ Ver.3 polymerase, Ex Taq™ polymerase, and Z-Taq™ polymerase were purchased from Takara Bio Inc. (Dalian, China). SYTO 9 and loading buffer were purchased from Thermo Fisher Scientific Inc. (Waltham, MA USA). The 50 bp DNA Ladder was purchased from Takara Bio Inc. (Dalian, China). Goldview fluorescent dye was purchased from SBS Genetech Co., Ltd. (Shanghai, China).

Transgenic soybean GTS 40-3-2 was kindly provided by the College of Life Sciences, Zhejiang University, Hangzhou, China; transgenic rice LL 601 was purchased from Monsanto Co., MO, USA; transgenic soybean DP 305423 and DP 356043 were purchased from DuPont Pioneer Hi-bred International, Inc., MA, USA; transgenic maize MON 810 was purchased from Monsanto Co. MO, USA; non-transgenic soybean, maize, rice, oilseed rape, potato and beet were purchased from the local market, Hangzhou, China.

Strains of *Vibrio parahaemolyticus* (ATCC33847), *Escherichia coli* O157:H7 (ATCC43889) *Saccharomyces cerevisiae* (CICC 1374), *Listeria monocytogenes* (ATCC 19151), *Escherichia coli* (ATCC25922), *Salmonella typhimurium* (ATCC 14028), *Escherichia coli* K12 (ATCC29425) and *Bacillus subtilis* (ATCC6633) were kindly provided by Zhejiang University, Hangzhou, China. The plasmid of *Infectious hypodermal and hematopoietic necrosis virus* was synthesized by Sangon Biotechnology Co., Ltd. (Shanghai, China).

The type-K insulated thermocouple (PN: 5TC-TT-K-40-36) was purchased from Omega Engineering Inc. (Norwalk, CA USA). The servo motor (PN: JX PDI-6221MG) was purchased from Jianxian Electronic Technology Co., Ltd. (Guangdong, China). The 3D printer was purchased from Flashforge Technology Co., Ltd. (Jinhua, China). The QuantStudio™ 3 Real-Time PCR System was purchased from Thermo Fisher Scientific Inc. (Waltham, MA USA). NanoDrop ND-1000 was purchased from Thermo Fisher Scientific Inc. (Waltham, MA USA). The thermo block and water baths were purchased from Aosheng Instrument Co., Ltd. (Hangzhou, China). The ChemiDoc XRS+ System was purchased from Bio-Rad Laboratories, Inc. (Hercules, CA USA).

### Heat transfer modeling analysis

Theoretical performance of plastic tube with 0.4/0.7 mm of inner/outer diameter was investigated by modeling analysis. It was based on one and two dimensional scenarios (1D and 2D). The heat was transferred from water bath to inside water (representing the reaction buffer of rapid PCR) through the thin wall of plastic tube. The temperature of water bath was regarded as constant (95 °C or 55 °C, respectively). **Table S1** listed the thermodynamic properties of plastic tube and water. The centerline inside plastic tube was the furthest location from water bath. It was regarded as adiabatic boundary condition without heat flux. The temperature distribution changes of plastic tube and inside water vs. time was simulated as **Figure S1-S3** displayed.

### Mock rapid PCR and real-time temperature measurement

Mock rapid PCR was conducted with the help of home-made rapid PCR amplification device (**Figure S4**). Briefly, the temperature inside plastic tube was monitored in real time via type-K insulated thermocouple.<sup>1,2</sup> The wire thermocouple probe was immersed and sealed inside the plastic tube that was filled with 40 μL of water. The temperature was measured and recorded every 0.01 s. During temperature measurement, mock rapid PCR was carried out under different conditions: 30 s hot start at 98 °C, followed by 40 cycles of [98 °C (1 s or 2 s or 5 s) and 55 °C (2 s or 3 s or 5 s)], respectively.

### DNA extraction and template preparation

GTS 40-3-2 soybean genomic DNA was extracted and purified by the TIANamp plant DNA kit according to its operation manual. Then, the extracted DNA was dissolved in 200 μL of tris-EDTA (TE) buffer and stored at -20 °C, with a concentration measured to be 14 ng μL<sup>-1</sup> by NanoDrop. Before sensitive detection assay, the stored soybean genomic DNA was gradually 10-fold diluted with sterile water to obtain template concentrations across 6 magnitudes. For rapid and traditional PCR amplification, 1 μL of DNA was used as template.

Similarly, the DNA of other plant samples were extracted and purified with TIANamp Plant DNA kit and stored at -20 °C. The DNA of bacteria samples were extracted and purified with TIANamp Bacteria DNA Kit and stored at -20 °C. The DNA of virus sample was extracted and purified with TIANamp Virus DNA/RNA Kit and stored at -20 °C.

### DNA copies theoretical calculation

The initial concentration of stock GTS 40-3-2 soybean genomic DNA was measured to be 14 ng μL<sup>-1</sup>. According to literature, the total complexity of soybean (*Glycine max*) genome is estimated to be 1115 Mbp.<sup>3</sup> Based on the formula, double strand DNA (ds DNA) copies=ds DNA concentration (ng μL<sup>-1</sup>)×6.02×10<sup>23</sup> ×10<sup>-9</sup> (660×bases)<sup>-1</sup>, the concentration of stock soybean genomic DNA was calculated to be approx. 1.16×10<sup>4</sup> copies per μL. Therefore, theoretically, the DNA copies of gradually diluted DNA templates were 1.16×10<sup>3</sup> copies (10-fold dilution), 1.16×10<sup>2</sup> copies (10<sup>2</sup>-fold dilution), 11.6 copies (10<sup>3</sup>-fold dilution), 1.16 copies (10<sup>4</sup>-fold dilution) and 0.12 copies (10<sup>5</sup>-fold dilution), respectively.

---

The initial concentration of stock LL601 rice genomic DNA was measured to be  $49.8 \text{ ng } \mu\text{L}^{-1}$ . The total complexity of rice genome is estimated to be 430 Mbp. Therefore, the concentration of LL601 rice genomic DNA was calculated to be approx.  $1.06 \times 10^5$  copies per  $\mu\text{L}$ . Therefore, theoretically, the DNA copies of gradually diluted LL601 rice genomic DNA templates were  $1.06 \times 10^4$  copies (10-fold dilution),  $1.06 \times 10^3$  copies ( $10^2$ -fold dilution),  $1.06 \times 10^2$  copies ( $10^3$ -fold dilution), 10.6 copies ( $10^4$ -fold dilution), 1.06 copies ( $10^5$ -fold dilution), respectively.

1 mL of *Vibrio parahaemolyticus* (ATCC33847) (approx.  $2.4 \times 10^6$  CFU  $\text{mL}^{-1}$ ) was used for DNA extraction and the DNA was dissolved in 200  $\mu\text{L}$  of tris-EDTA (TE) buffer. Therefore, the initial concentration of *Vibrio parahaemolyticus* (ATCC33847) DNA was  $1.2 \times 10^4$  copies per  $\mu\text{L}$ . Therefore, theoretically, the DNA copies of gradually diluted *Vibrio parahaemolyticus* (ATCC33847) DNA templates were  $1.2 \times 10^3$  copies (10-fold dilution),  $1.2 \times 10^2$  copies ( $10^2$ -fold dilution), 12 copies ( $10^3$ -fold dilution), 1.2 copies ( $10^4$ -fold dilution), respectively. Similarly, the initial concentration of *Infectious hypodermal and hematopoietic necrosis virus* DNA was calculated to be  $1.8 \times 10^4$  copies per  $\mu\text{L}$ . Therefore, with 10-fold gradually dilution, the concentration of *infectious hypodermal and hematopoietic necrosis virus* DNA templates were approx.  $1.8 \times 10^3$  copies (10-fold dilution),  $1.8 \times 10^2$  copies ( $10^2$ -fold dilution), 18 copies ( $10^3$ -fold dilution), 1.8 copies ( $10^4$ -fold dilution), respectively.

### **Amplicon counting process with modified rapid PCR**

The reaction solution with 1  $\mu\text{L}$  of soybean genomic DNA as template was prepared and mixed thoroughly. Then, the reaction solution was injected into plastic tube and the open ends were sealed with flame. Next, the sealed plastic tube was shuttled between two water baths with the help of home-made device for a serial process of denaturation and annealing/extension. After rapid DNA amplification for 45 cycles within 5 min, the plastic tube was placed under the UV light. The image of amplicon cluster in plastic tube could be observed by naked eye. At the same time, the amount of target DNA molecules could be obtained by counting the number of amplicon cluster segments.

### **Gel electrophoresis and imaging**

After PCR amplification, 1  $\mu\text{L}$  of DNA amplicon was mixed with 2  $\mu\text{L}$  of loading buffer and electrophoresed on a 3 % (*w/v*) agarose gel. The whole gel process was conducted at constant voltage of 110 V for 35 min. A 50 bp DNA Ladder was used for amplicon size control. Then, the agarose gel was supplemented with Goldview in TAE buffer solution for 30 min. Thereafter, the gel was imaged and photographed with ChemiDoc XRS+ System.

---

## Results and Discussion

### Heat transfer modeling analysis

Based on the thermal conductivity and specific heat capacity of water and plastic tube (**Table S1**), a numerical model was developed to predict the temperature distribution changes with time extension for the plastic tube and inside water. To simply the modeling process, a symmetric half model was conducted by using an adiabatic boundary condition to the centerline of the plastic tube (**Figure S1**). The simulation parameters were set to mimic plastic tube with wall thickness of 0.15 mm and inner radius of 0.2 mm. The initial temperature of plastic tube and inside water was 95 °C. The temperature of water bath was uniform and constant at 55 °C.

As **Figure S2** illustrated, when plastic tube immersed in water bath, its outer wall was heated immediately. The simulation showed that in the first 0.05 s, the outer wall temperature of plastic tube increased approx. 12 °C. Soon afterwards, the temperature of inside plastic tube increased through conduction. Results demonstrated that the inner wall-water interface temperature increased to 60 °C after 0.1 s. After 3 s, the system equilibrated to the temperature of water bath with 95% equilibrium. Additionally, the heat transfer system was also modeled as 2D conduction of 55 °C plastic tube equilibrating temperature with constant 95 °C of water bath. The images presented the temperature distribution changes of plastic tube and inside water with 0.1 s of interval. The red color represented high temperature and brown color represented low temperature. Results indicated that the periphery of plastic tube was firstly heated, following by the inner of plastic tube. Soon afterwards, the water inside plastic tube was heated through conduction. The plastic tube system equilibrated to the temperature of water bath within 3 s.

Similarly, when the temperature of plastic tube and inside water was initially uniform at 55 °C with constant temperature of water bath at 95 °C, the plastic tube system could also equilibrated to the temperature of water bath with 95% equilibrium within 3s (**Figure S3**).

---

**Table S1** Thermodynamic properties of materials.<sup>4,5</sup>

<b>Material</b>	<b>Conductivity, <math>k</math> (<math>\text{Wm}^{-1}\text{K}^{-1}</math>)</b>	<b>Density, <math>\rho</math> (<math>\text{kgm}^{-3}</math>)</b>	<b>Specific heat capacity, <math>c_p</math> (<math>\text{Jkg}^{-1}\text{K}^{-1}</math>)</b>
Water	0.6	1000	4180
Polypropylene (PP)	0.21	900	1930

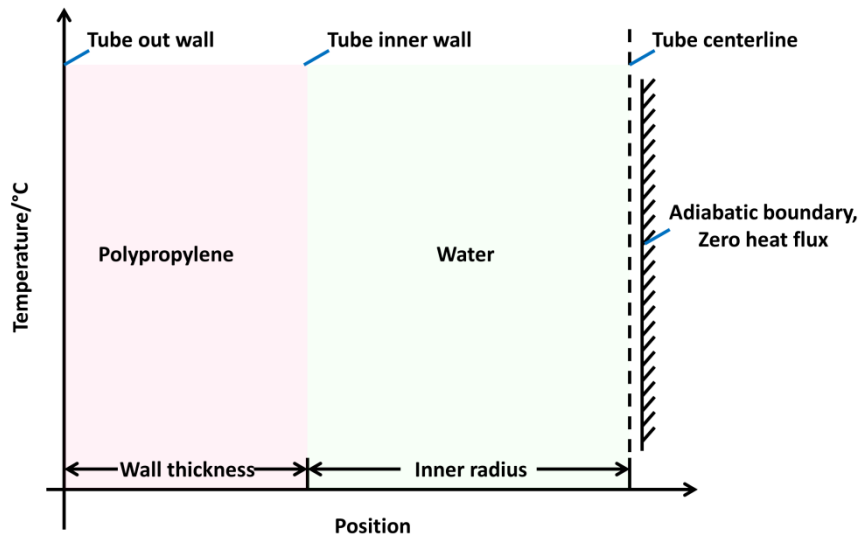
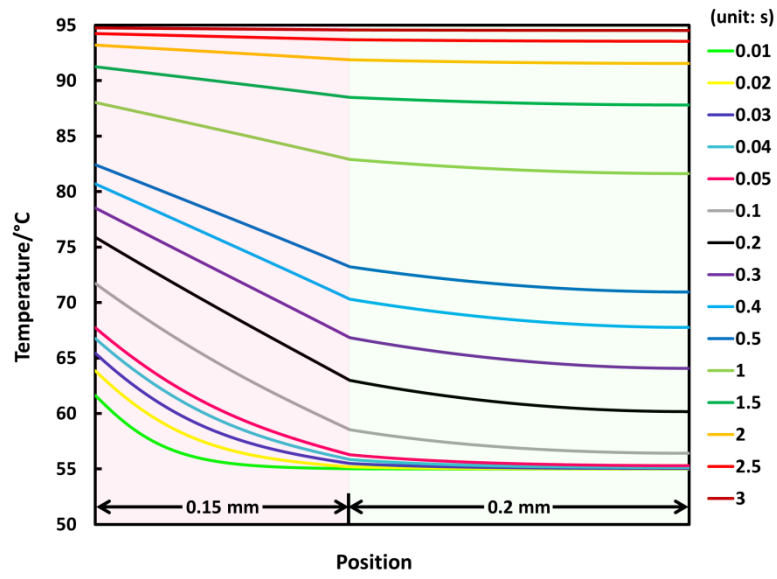


**Figure S1** Numerical simulation condition. For boundary condition, the heat flux was set to be zero at the centerline of plastic tube. In the initial, the plastic tube and inside water were at the same temperature. The horizontal axis presented the thickness of plastic tube wall and the inner radius of plastic tube. Simulation tracked the temperature distribution changes of plastic tube and inside water with time extension.

(a)



(b)

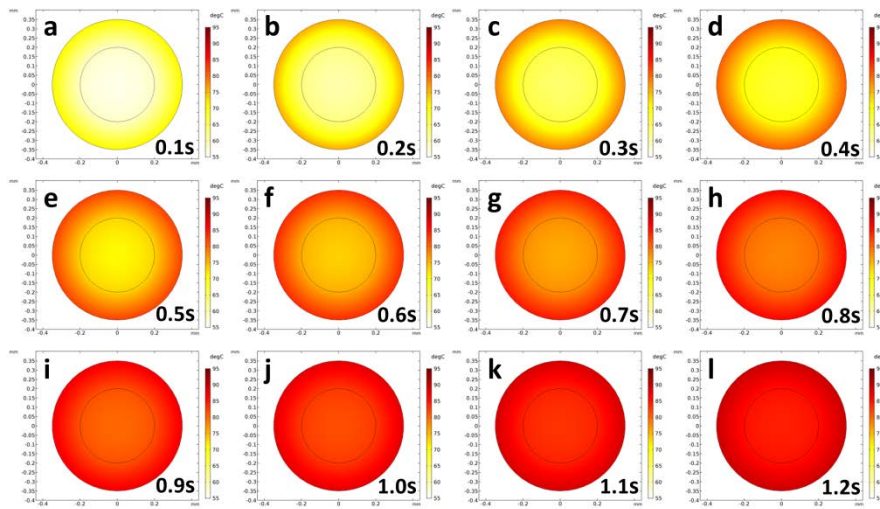
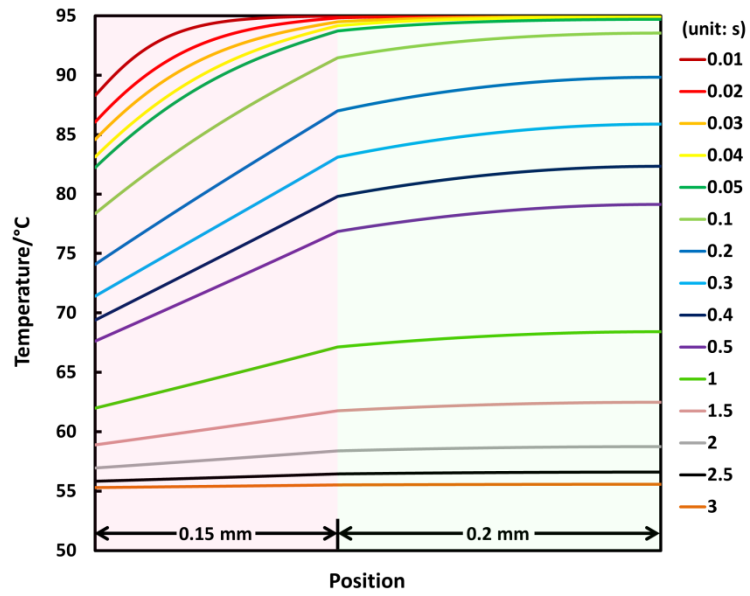


**Figure S2** Numerical and 2D simulation results of temperature distribution changes vs. time for the plastic tube and inside water. The temperature of plastic tube and inside water was initially uniform at 55 °C with constant temperature of water bath at 95 °C.

(a)



(b)

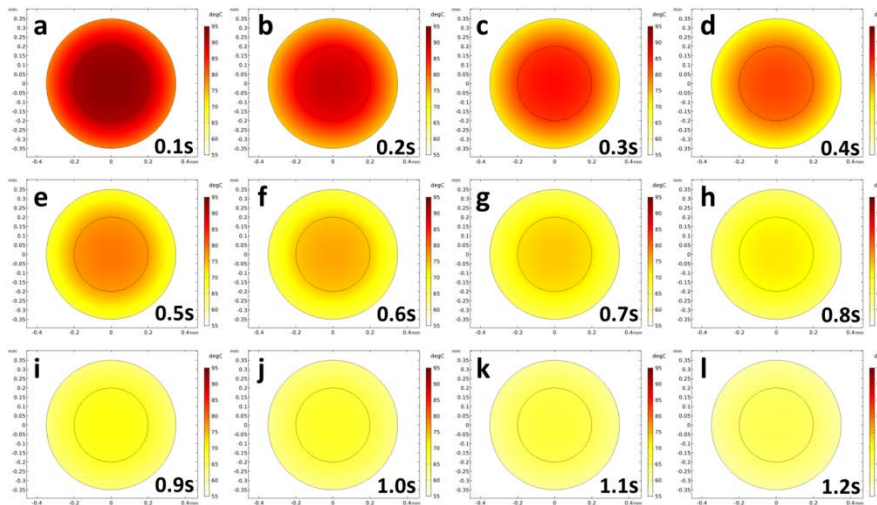


**Figure S3** Numerical and 2D simulation results for the plastic tube and inside water. The initial temperature of plastic tube and inside water was 95 °C. The temperature of water bath was uniform and constant at 55 °C.

---

## Mock rapid PCR

Mock rapid PCR was carried out for 40 thermo cycles under following conditions: 30 s hot start at 98 °C, followed by 40 cycles of [98 °C (1 s or 2s or 5 s) and 55 °C (2 s or 3s or 5 s)], respectively. **Figure S5** displayed the temperature profile with inset illustrated an expanded view for a couple of thermo cycles. Results in **Figure S5a** showed that, for 3 s per cycle process, the trace of temperature presented peak shapes. The maximum and minimum temperatures attained during each PCR cycle varied and could not reach the temperature of water baths. For 5s per cycle process, the average denaturation and annealing/extension temperatures attained with such apparatus during each PCR cycle were  $96 \pm 0.61$  °C and  $56 \pm 0.28$  °C, respectively (**Figure S5b**). When 10 s per cycle was conducted, plateaus generated during denaturation and annealing/extension processes. The plateaus for annealing/extension (between 60 °C and 55 °C) and denaturation (above 90 °C) were lasted 4.11 s and 3.84 s, respectively (**Figure S5c**). Using the thermo cycling result, heating and cooling rates were calculated by derivation. The maximum heating/cooling ramp rates were both around  $35$  °C $s^{-1}$ .

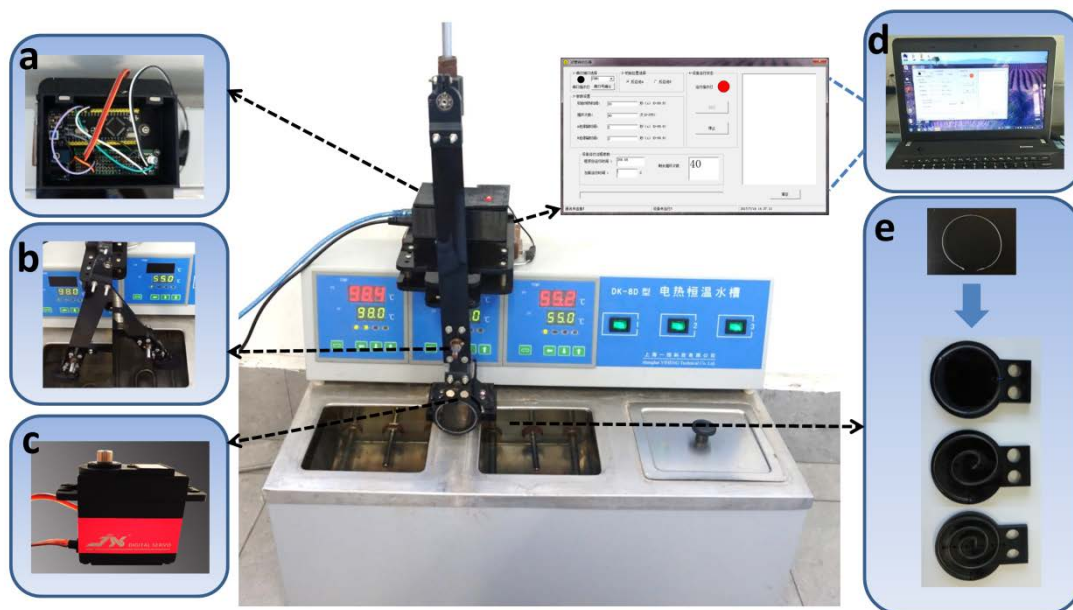
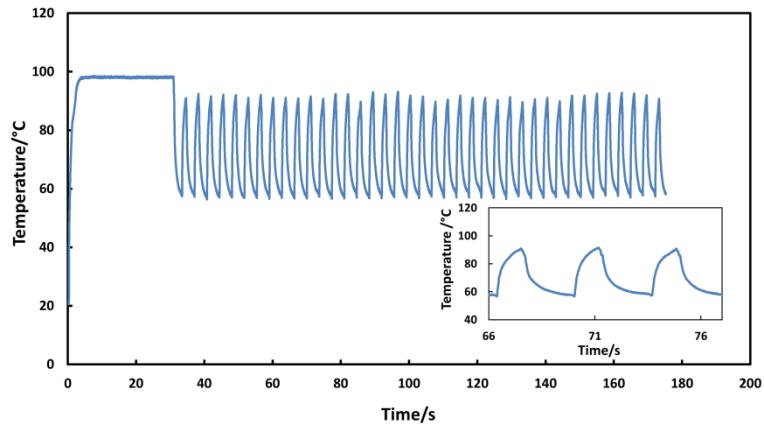
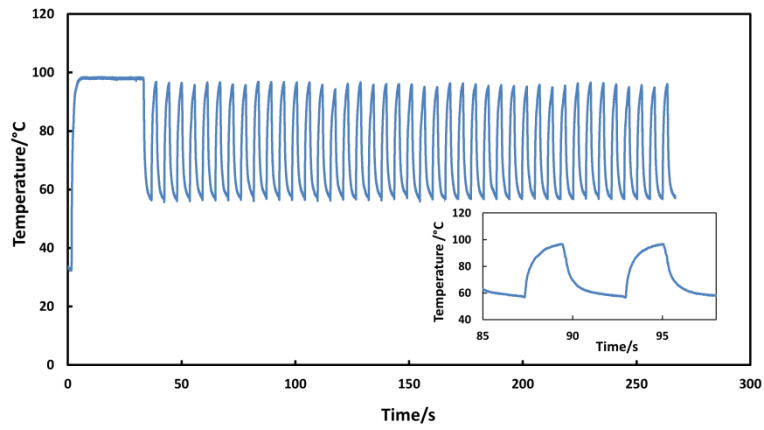


**Figure S4.** The home-made device for rapid PCR amplification. It contains a control circuit (a) connected with the servo motor (c) to auto-control the mechanical arm (b) shuttling between the two water baths. The sealed plastic tube (e) that containing reaction mixture was fixed on the 3D printing model (e) and assembled on the mechanical arm for rapid PCR amplification through thermo cycling. A LabView program controlled stepper motion was developed to obtain the desired thermo cycling progress. The control interface was as (d) shown.

(a)



(b)



(c)

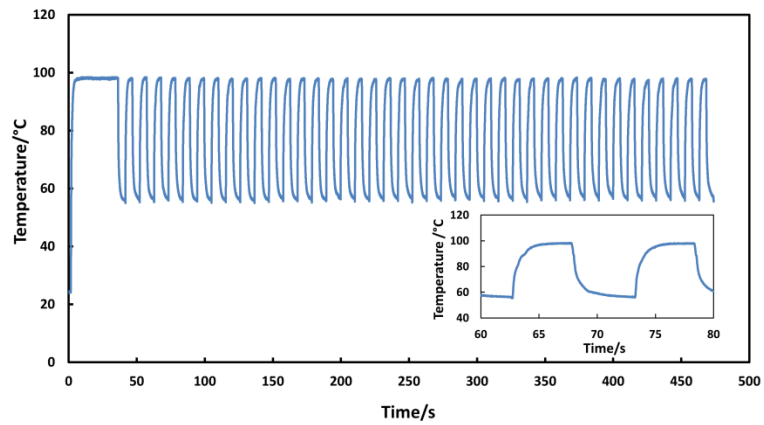


**Figure S5** Thermal trace showing around 40 cycles of rapid PCR with inset showing an expanded view of a few cycles. Rapid PCR was performed with various conditions: 30 s hot start at 98 °C, followed by 40 cycles of [98 °C (1 s or 2s or 5 s) and 55 °C (2 s or 3s or 5 s)] as shown in (a), (b) and (c), respectively.

---

## Investigation of rapid PCR amplification

We assessed the performance of rapid PCR amplification with different product lengths and DNA polymerases. Five kinds of enzyme, Taq<sup>TM</sup> polymerase, SpeedSTAR<sup>TM</sup> polymerase, MightyAmp<sup>TM</sup> Ver.3 polymerase, Ex Taq<sup>TM</sup> polymerase, and Z-Taq<sup>TM</sup> polymerase were employed in this paper. The template lengths were 165, 220, 354, 449, 549, 617 bp, respectively. Rapid PCR was performed with the following conditions: 30 s hot start at 98 °C, followed by 45 cycles of [98 °C (1 s or 2 s or 5 s) and 55°C (2 s or 3 s or 5 s)], which were 3 s per cycle, 5 s per cycle and 10 s per cycle, respectively.

Results in **Figure S6a-S10a** indicated that, under the condition of 3 s per cycle, 165 bp fragments could only be amplified by SpeedSTAR<sup>TM</sup> polymerase. When the thermo cycling time extended to 5 s per cycle, 165 bp products could be determined by all the other ones except MightyAmp<sup>TM</sup> Ver.3 polymerase (**Figure S6b-S10b**). Moreover, when the extension time was 3 s for each cycle, the 220 bp templates could also be successfully amplified by SpeedSTAR<sup>TM</sup> polymerase and Z-Taq<sup>TM</sup> polymerase, which featured both of them with outstanding extension speed (**Figure S7b and S10b**). When 10 s per cycle was conducted for rapid PCR amplification, all products  $\leq 220$  bp displayed obvious bands at the right locations in the gel image (**Figure S6c-S10c**). Additionally, the 354 bp product could be detected by SpeedSTAR<sup>TM</sup> polymerase and Z-Taq<sup>TM</sup> polymerase (**Figure S7c and S10c**), while the 449 bp segment could only be successfully amplified by SpeedSTAR<sup>TM</sup> polymerase (**Figure S7c**). No amplification was observed in all no-template controls (NTCs). Results indicated that as the fragment size increases, longer annealing/extension times were needed for complete extension. After comparison, the extension efficiency of SpeedSTAR<sup>TM</sup> polymerase is highest, followed by Z-Taq<sup>TM</sup> polymerase. Taq<sup>TM</sup> polymerase, Ex Taq<sup>TM</sup> polymerase displayed equal amplification efficiency, while MightyAmp<sup>TM</sup> Ver.3 polymerase showed lowest extension efficiency. Hence, product lengths and extension speed of polymerase should be taken into consideration before rapid PCR amplification.

To further determine the amplification accuracy, the amplicon of rapid PCR with various template concentrations were sequenced (**Figure S12**). All the sequencing and blast results demonstrated that rapid PCR amplification owns as high as 99% amplification accuracy. Therefore, rapid PCR could be conducted with different DNA polymerases, presenting high amplification specificity and accuracy, as well as robust applicability for while-you-wait testing.

**Table S2.** The targets, primer sequences and corresponding product sizes used in this study.

Gene	Primer name	Sequence (5'-3')	Primer length (bp)	Target length (bp)
<i>T-nos</i>	F I	ATCGTTCAAACATTGGCA	19	165
	R I	ATTGCGGGACTCTAATCATA	20	
<i>CP4EPSPS</i>	F II	AGGAAGGTGGCTCCTACAAATGC	23	220
	R II	GAAGGGTCTTGCGAAGGATAGTG	23	
<i>tlh</i>	F III	GACATTACGTTCTTCGCCGC	20	354
	R III	GTTCTTCGCCAGTTTTCGCT	20	
<i>tlh</i>	F IV	AAGCGGATTATGCAGAAGCACTG	23	449
	R IV	GCTACTTCTAGCATTCTCTGC	24	
<i>CP4EPSPS</i>	F V	ACAAACCCCTAATCCCAATTCCA	23	549
	R V	TCGCCGATGAAGGTGCTGTC	20	
<i>CP4EPSPS</i>	F VI	GTTGCGCCCTGCTTGTTC	20	617
	R VI	GCTCATCAGGCAGCCTTCGTAT	22	
<i>CaMV35S</i>	F VII	CGACAGTGGTCCCAAAGA	18	74
	R VII	AAGACGTGGTTGGAACGTCTTC	22	
<i>tlh</i>	F VIII	ACCATTGACGGCTACTGGTG	20	142
	R VIII	CAGCGGCGAAGAACGTAATG	20	
<i>IHHNV</i>	F IX	CGGAACACAACCCGACTTTA	20	389
	R IX	GGCCAAGACCAAATACGAA	20	

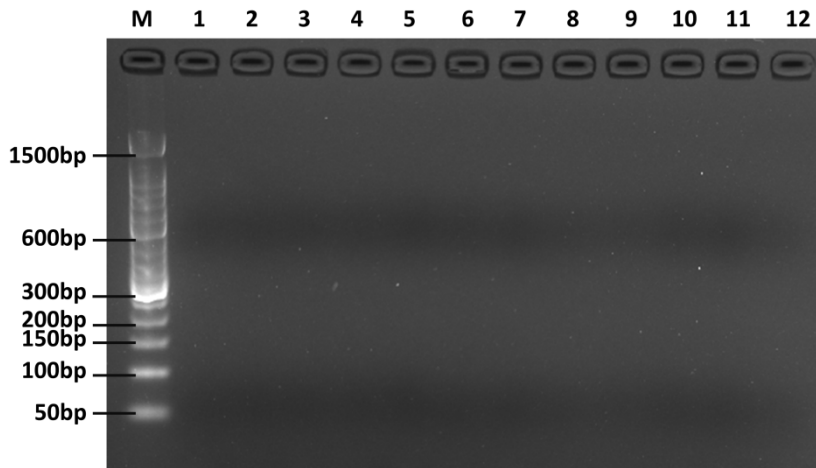
Note: *Agrobacterium tumefaciens* nopaline synthase terminator (*T-nos*, GenBank No. KX683862.1); Roundup Ready gene (*CP4EPSPS*, GenBank No. AB209952.1). Both *T-nos* gene and *CP4EPSPS* gene are genomic elements in GTS 40-3-2 soybean samples. *V. parahaemolyticus*-specific *thermolabile haemolysin* gene (*tlh*, GenBank No. M36437). *Cauliflower mosaic virus* 35S promoter (*CaMV35S*, GenBank No. GU734659.1). *Infectious hypodermal and hematopoietic necrosis virus* complete genome (*IHHNV*, GenBank No. AF218266). Primer I and VII, respectively for *T-nos* and *CaMV 35S* detection, were cited according to GB 953-6-2007, Primer IX for *IHHNV* detection was cited according to GB/T 25878-2010

**Table S3.** Reaction conditions of rapid and traditional PCR used in this paper.

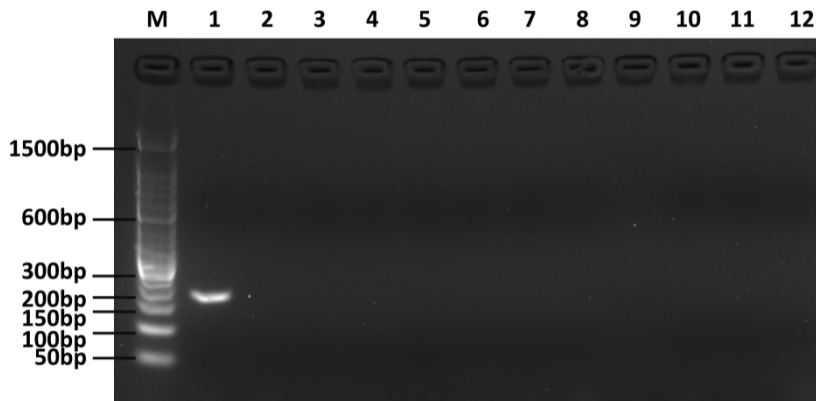
Reagent	Work concentration	
	Rapid PCR	Traditional PCR
DNA polymerase*	10 U	1 U
Tris HCl (pH 8.3)	10 mM	10 mM
KCl	50 mM	50 mM
MgCl <sub>2</sub>	1.5 mM	1.5 mM
dNTP (each)	0.2 mM	0.2 mM
Forward primer	0.4 $\mu$ M	0.4 $\mu$ M
Reverse primer	0.4 $\mu$ M	0.4 $\mu$ M
SYTO 9*	8 $\mu$ M	2 $\mu$ M
Template	1 $\mu$ L	1 $\mu$ L
Sterile water	Up to 40 $\mu$ L	Up to 40 $\mu$ L

\*To implement rapid PCR amplification, the concentration of DNA polymerase used is 9 times higher than that of traditional PCR. We found that SYTO 9 with the concentration of 8  $\mu$ M was optimal for visual observation and DNA molecules counting after rapid PCR amplification.

(a)



(b)



(c)

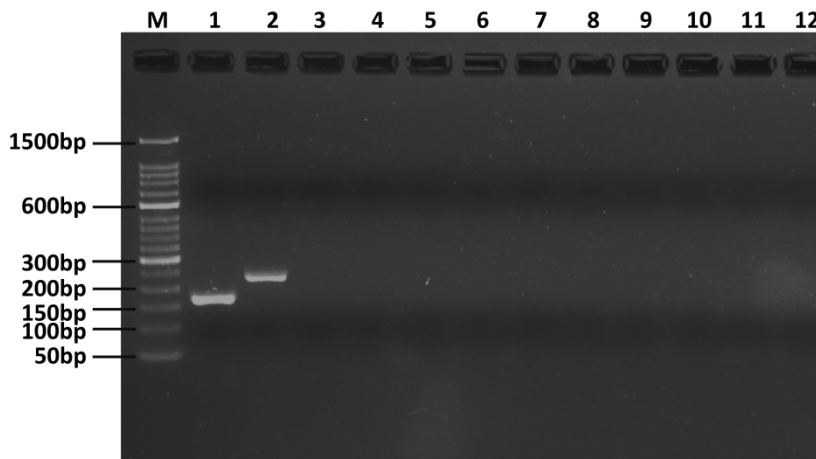
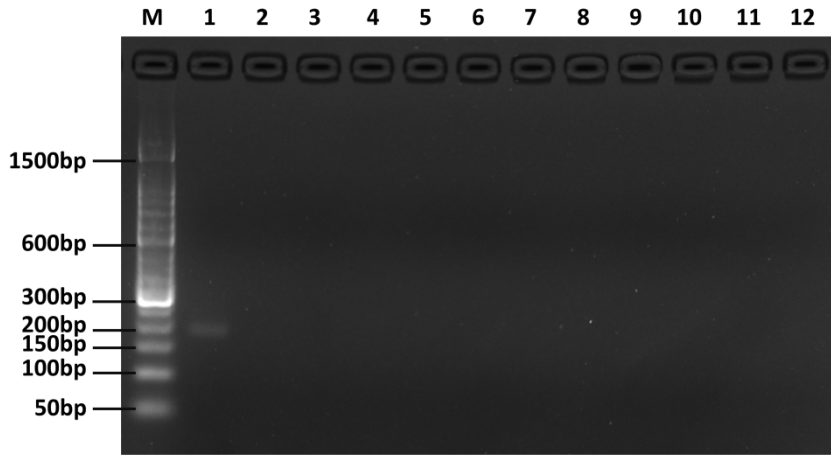
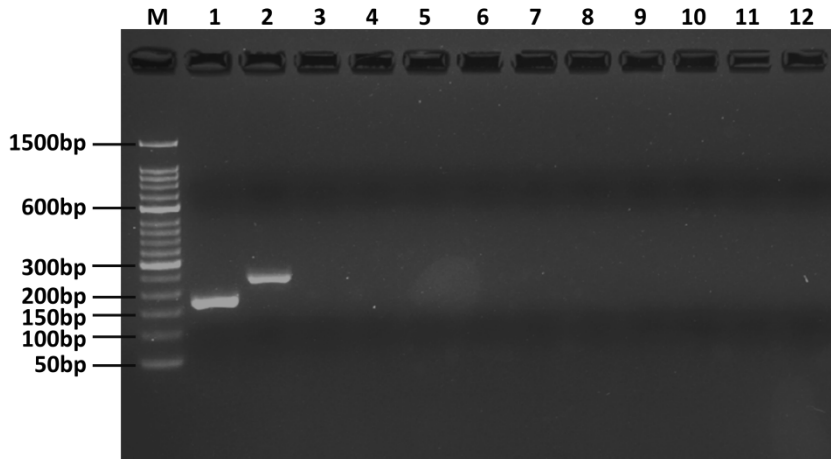


**Figure S6** Rapid PCR amplification with Taq™ polymerase. Target DNA used in this study were in the length of 165 bp (lane 1), 220 bp (lane 2), 354 bp (lane 3), 449 bp (lane 4), 549 bp (lane 5), 617 bp (lane 6), with no template added as negative control (lanes 7-12), respectively. Different rapid PCR amplification processes were conducted with 3 s per cycle (a), 5 s per cycle (b) and 10 s per cycle (c), respectively.

(a)



(b)



(c)

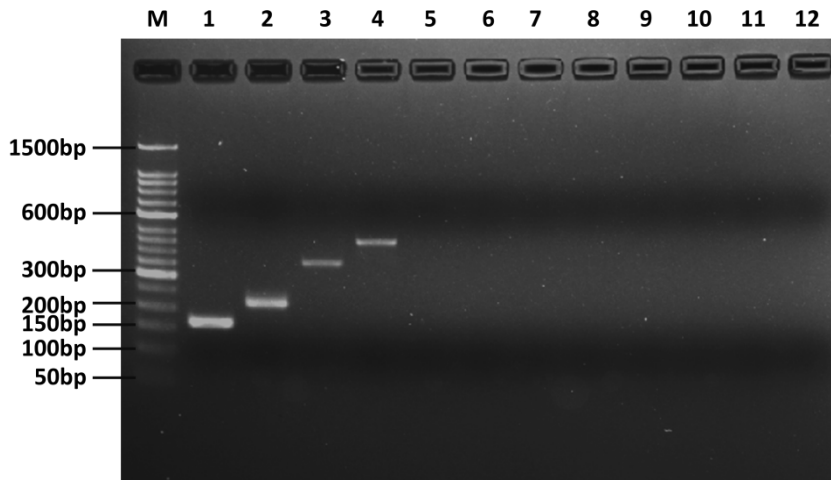
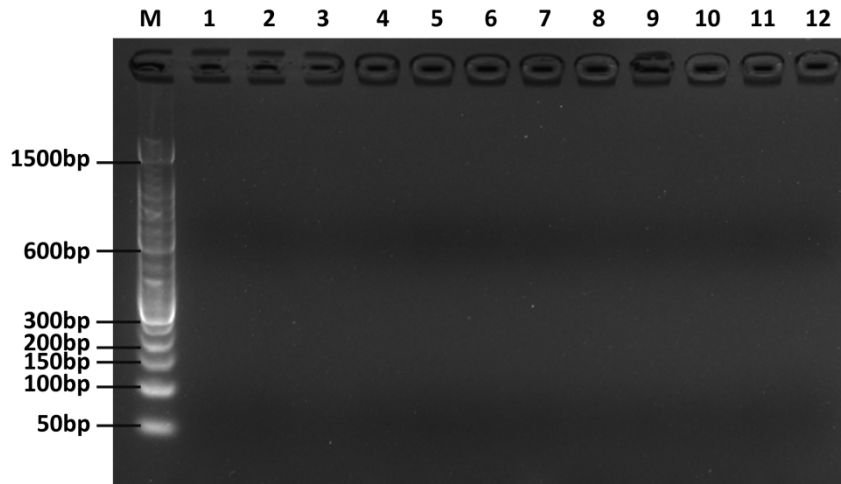
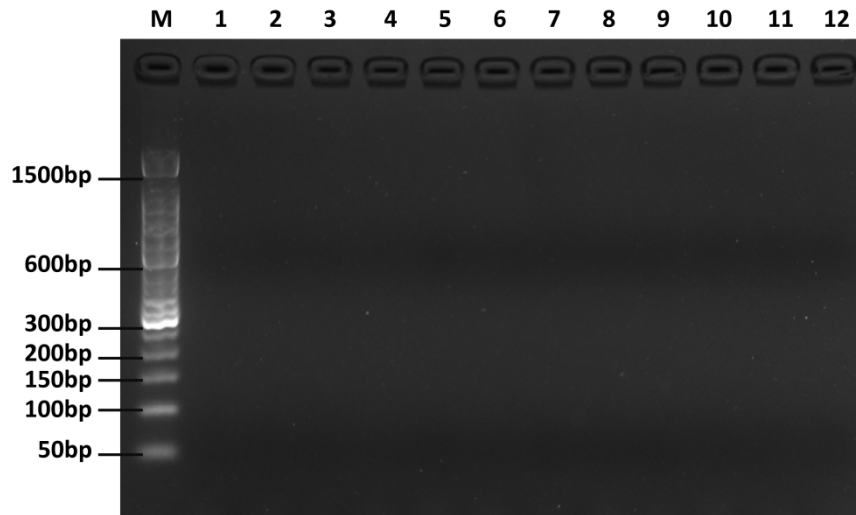


**Figure S7** Rapid PCR amplification with SpeedSTAR™ polymerase. Target DNA used in this study were 165 bp (lane 1), 220 bp (lane 2), 354 bp (lane 3), 449 bp (lane 4), 549 bp (lane 5), 617 bp (lane 6), with no template added as negative control (lanes 7-12), respectively. Different rapid PCR amplification processes were conducted with 3 s per cycle (a), 5 s per cycle (b) and 10 s per cycle (c), respectively.

(a)



(b)



(c)

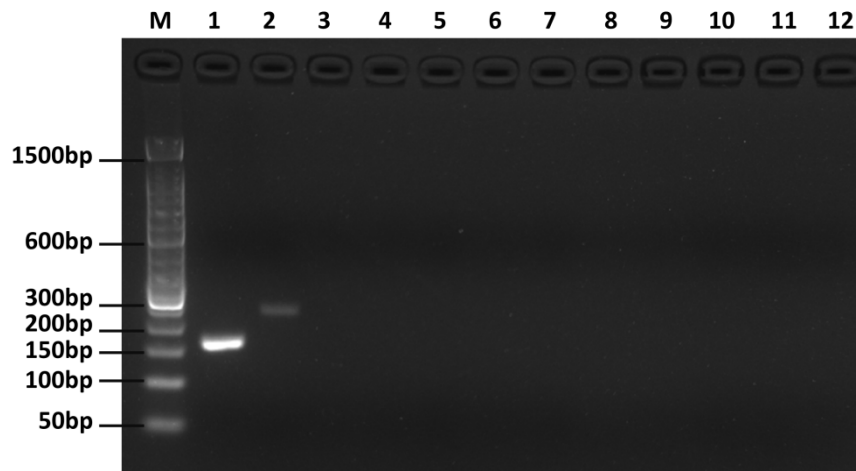
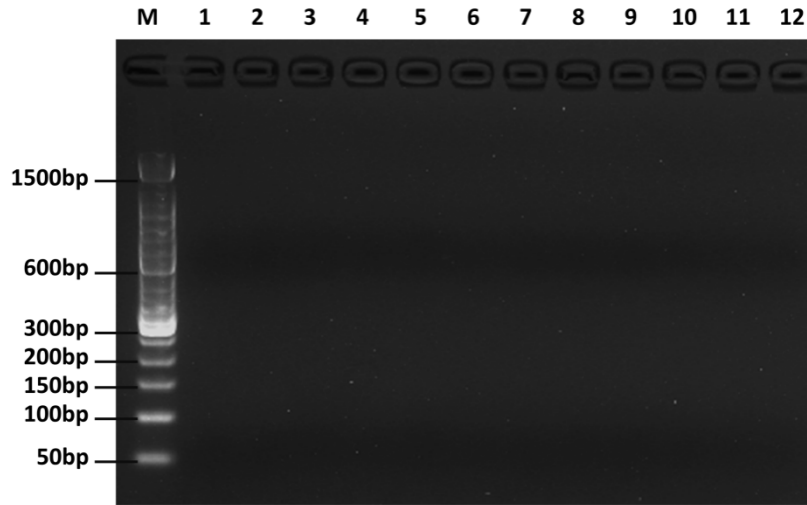
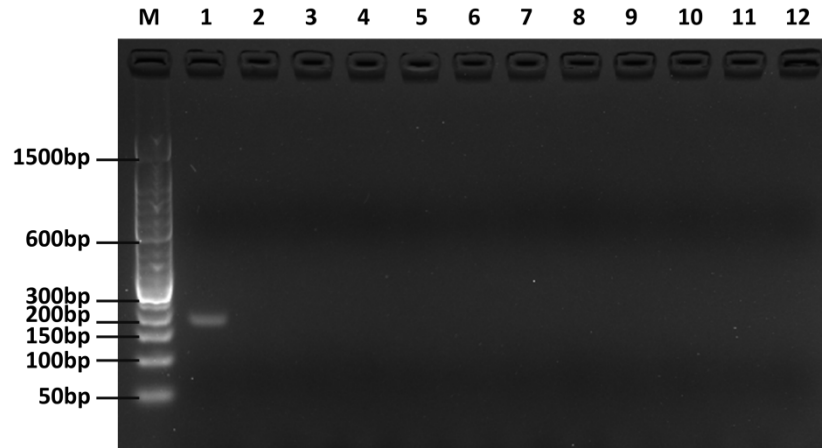


**Figure S8** Rapid PCR amplification with MightyAmp™ Ver.3 polymerase. Target DNA used in this study were 165 bp (lane 1), 220 bp (lane 2), 354 bp (lane 3), 449 bp (lane 4), 549 bp (lane 5), 617 bp (lane 6), with no template added as negative control (lanes 7-12), respectively. Different rapid PCR amplification processes were conducted with 3 s per cycle (a), 5 s per cycle (b) and 10 s per cycle (c), respectively.

(a)



(b)



(c)

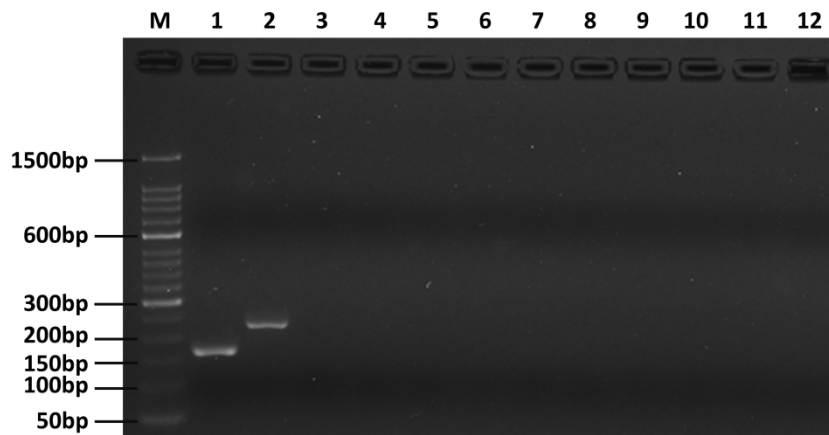
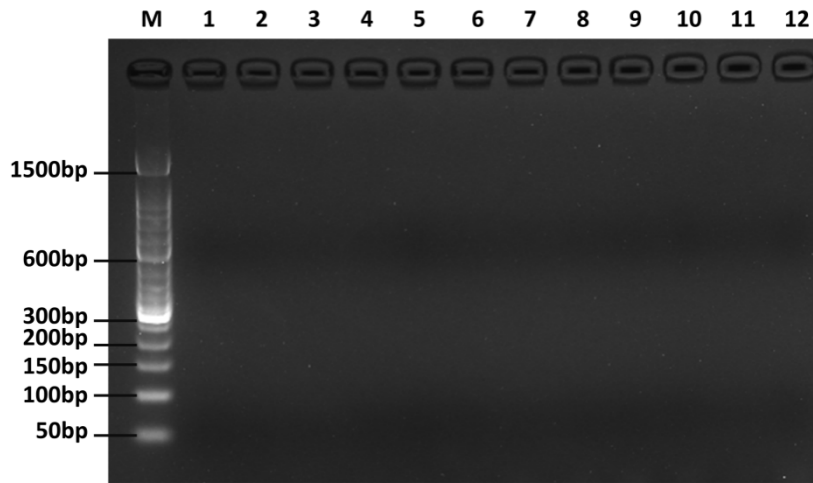
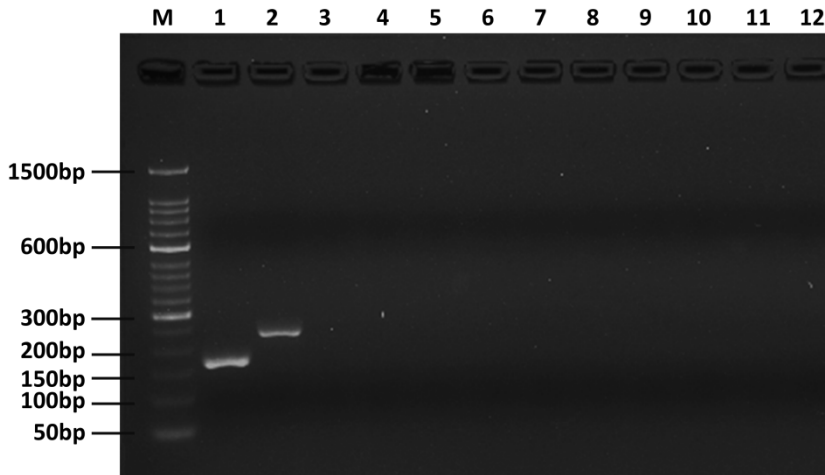


**Figure S9** Rapid PCR amplification with Ex Taq™ polymerase. Target DNA used in this study were 165 bp (lane 1), 220 bp (lane 2), 354 bp (lane 3), 449 bp (lane 4), 549 bp (lane 5), 617 bp (lane 6), with no template added as negative control (lanes 7-12), respectively. Different rapid PCR amplification processes were conducted with 3 s per cycle (a), 5 s per cycle (b) and 10 s per cycle (c), respectively.

(a)



(b)



(c)

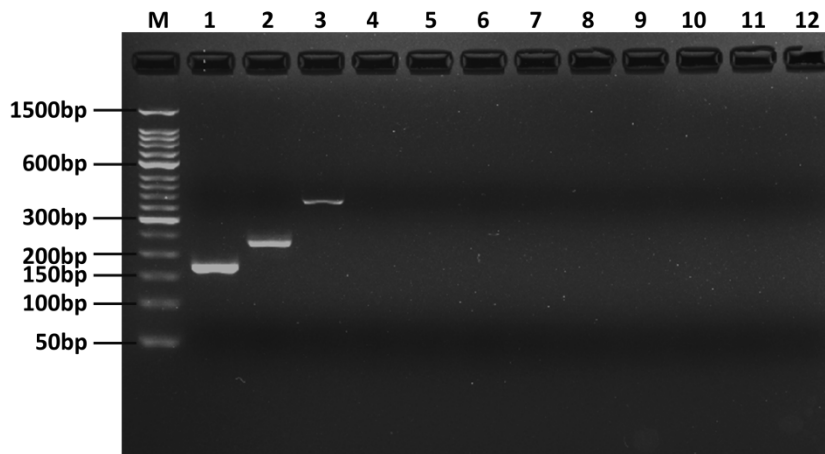


**Figure S10** Rapid PCR amplification with Z-Taq™ polymerase. Target DNA used in this study were 165 bp (lane 1), 220 bp (lane 2), 354 bp (lane 3), 449 bp (lane 4), 549 bp (lane 5), 617 bp (lane 6), with no template added as negative control (lanes 7-12), respectively. Different rapid PCR amplification processes were conducted with 3 s per cycle (a), 5 s per cycle (b) and 10 s per cycle (c), respectively.

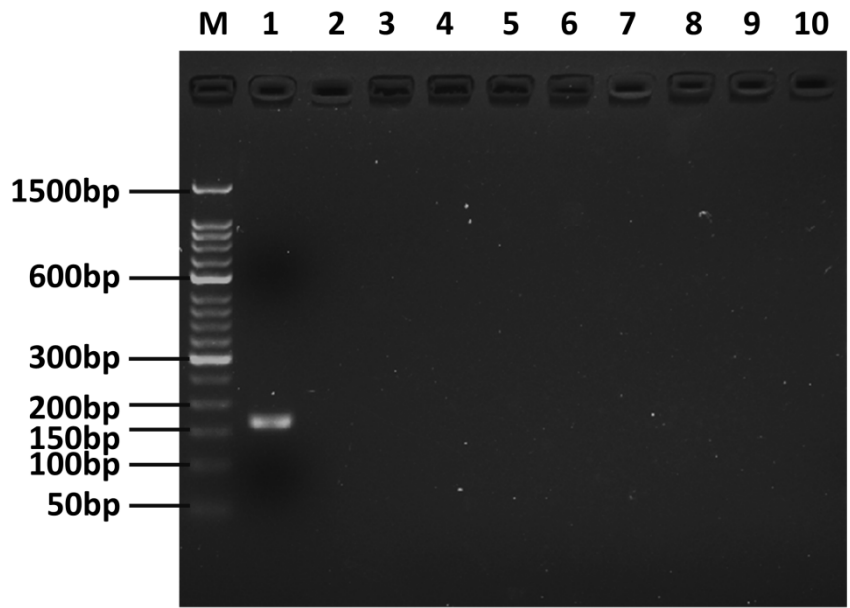
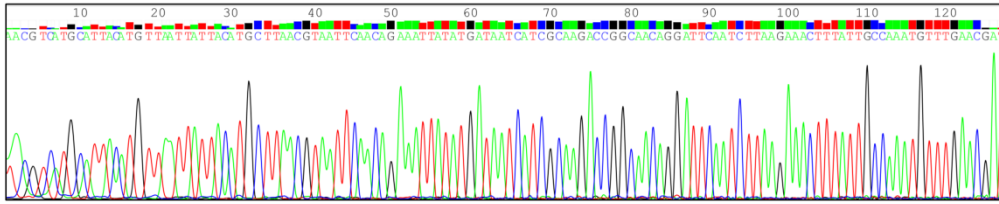


**Figure S11** Detection specificity of rapid PCR amplification in capillary for *T-nos* gene determination. From lane 1-10, the tested samples were GTS 40-3-2 soybean, DP 305423 soybean, DP 356043 soybean, MON 810 maize, non-transgenic soybean, maize, rice, oilseed rape, potato and beet, respectively. M, 50 bp DNA ladder.

(a)



Binary vector pAGW633, complete sequence

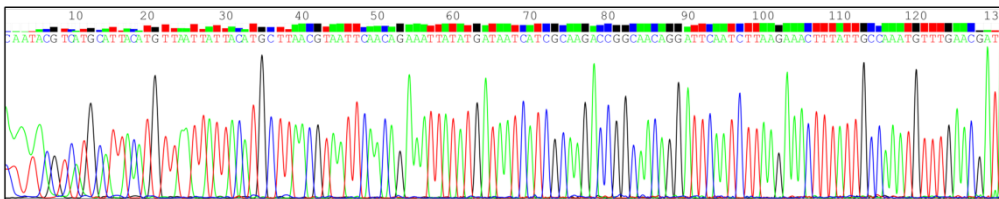
Sequence ID: [KX683862.1](#) Length: 10326 Number of Matches: 2

Range 1: 3915 to 4041 [GenBank](#) [Graphics](#)

▼ Next Match ▲ Previous Match

Score	Expect	Identities	Gaps	Strand
235 bits(127)	2e-58	127/127(100%)	0/127(0%)	Plus/Plus
Query 1	AACGTCATGCATTACATGTTAATTATTACATGCTTAACGTAATTCAACAGAAATATATG	60		
Sbjct 3915	AACGTCATGCATTACATGTTAATTATTACATGCTTAACGTAATTCAACAGAAATATATG	3974		
Query 61	ATAATCATCGCAAGACCGGCAACAGGATCAATCTTAAGAAACTTTATTGCCAAATGTTT	120		
Sbjct 3975	ATAATCATCGCAAGACCGGCAACAGGATCAATCTTAAGAAACTTTATTGCCAAATGTTT	4034		
Query 121	GAACGAT	127		
Sbjct 4035	GAACGAT	4041		

(b)



Binary vector pAGW633, complete sequence

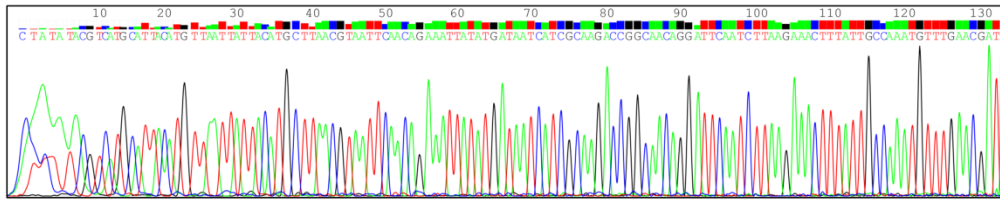
Sequence ID: [KX683862.1](#) Length: 10326 Number of Matches: 2

Range 1: 3912 to 4041 [GenBank](#) [Graphics](#)

▼ Next Match ▲ Previous Match

Score	Expect	Identities	Gaps	Strand
233 bits(126)	6e-58	129/130(99%)	1/130(0%)	Plus/Plus
Query 2	AAT-ACGTCATGCATTACATGTTAATTATTACATGCTTAACGTAATTCAACAGAAATAT	60		
Sbjct 3912	AATAACGTCATGCATTACATGTTAATTATTACATGCTTAACGTAATTCAACAGAAATAT	3971		
Query 61	ATGATAATCATCGCAAGACCGGCAACAGGATCAATCTTAAGAAACTTTATTGCCAAATG	120		
Sbjct 3972	ATGATAATCATCGCAAGACCGGCAACAGGATCAATCTTAAGAAACTTTATTGCCAAATG	4031		
Query 121	TTTGAACGAT	130		
Sbjct 4032	TTTGAACGAT	4041		

(c)



Binary vector pAGW633, complete sequence

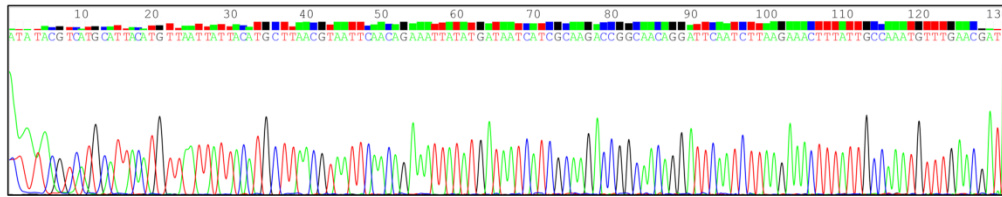
Sequence ID: [KX683862.1](#) Length: 10326 Number of Matches: 2

Range 1: 3913 to 4041 [GenBank](#) [Graphics](#)

▼ Next Match ▲ Previous Match

Score	Expect	Identities	Gaps	Strand
233 bits(126)	6e-58	129/130(99%)	1/130(0%)	Plus/Plus
Query 3	ATATACGTCATGCATTACATGTTAATTATTACATGCTTAACGTAATCAACAGAAATTAT	62		
Sbjct 3913	ATA-ACGTCATGCATTACATGTTAATTATTACATGCTTAACGTAATCAACAGAAATTAT	3971		
Query 63	ATGATAATCATCGCAAGACCGGCAACAGGATTCAATCTTAAGAAACTTTATTGCCAAATG	122		
Sbjct 3972	ATGATAATCATCGCAAGACCGGCAACAGGATTCAATCTTAAGAAACTTTATTGCCAAATG	4031		
Query 123	TTTGAACGAT	132		
Sbjct 4032	TTTGAACGAT	4041		

(d)



Binary vector pAGW633, complete sequence

Sequence ID: [KX683862.1](#) Length: 10326 Number of Matches: 2

Range 1: 3913 to 4041 [GenBank](#) [Graphics](#)

▼ Next Match ▲ Previous Match

Score	Expect	Identities	Gaps	Strand
233 bits(126)	6e-58	129/130(99%)	1/130(0%)	Plus/Plus
Query 1	ATATACGTCATGCATTACATGTTAATTATTACATGCTTAACGTAATCAACAGAAATTAT	60		
Sbjct 3913	ATA-ACGTCATGCATTACATGTTAATTATTACATGCTTAACGTAATCAACAGAAATTAT	3971		
Query 61	ATGATAATCATCGCAAGACCGGCAACAGGATTCAATCTTAAGAAACTTTATTGCCAAATG	120		
Sbjct 3972	ATGATAATCATCGCAAGACCGGCAACAGGATTCAATCTTAAGAAACTTTATTGCCAAATG	4031		
Query 121	TTTGAACGAT	130		
Sbjct 4032	TTTGAACGAT	4041		

**Figure S12** Sequencing and blast results of rapid PCR amplification with various template concentrations. Soybean genomic DNA as template for each sample was with stock concentration (a) or after 10-fold (b),  $10^2$ -fold (c) and  $10^3$ -fold dilutions (d), respectively.

---

## Counting DNA molecules with rapid PCR

After rapid PCR amplification, amplicon cluster segments inside plastic tube were imaged under UV light. The amount of amplicon cluster segments in each sample was counted and regarded as the number of template molecules. Based on our results, the size of amplicon cluster was approx. 3 mm. However, there were four samples with amplicon cluster size far beyond 3 mm, as **Figure S13** displayed. We assume this was due to DNA molecules flocked together in plastic tube before rapid PCR amplification.

To verify the consistency of obtained amplicon cluster segments number and the initial amounts of template DNA molecules, rapid PCR reaction with different concentration of templates has been conducted. Results in **Figure S14** demonstrated that there were no amplicon cluster segments for NTCs. With the increase of DNA template concentration, the number of amplicon cluster segments in plastic tube was also increased. When the template concentration was equal to or above  $10^2$ -fold dilutions, the whole plastic tube turned bright. Therefore, the amplicon cluster segments were amplified by DNA templates and their number could be counted if DNA template at a low concentration.

The diffusion processes of amplicon cluster at room temperature were illustrated as **Figure S15**. Each sample was imaged under UV light right after standing for 0, 2, 4, 6 and 12 h, respectively. As is shown, the sizes of amplicon clusters were almost the same after as long as 2 h standing, representing extremely low diffusion efficiency of amplicon clusters in thin plastic tube. With the standing time extension, amplicon clusters gradually diffused. The whole diffusion process could also be seen in the **Flash in ESI**. Based on the size change of amplicon cluster vs. time, the diffusion coefficient ( $D$ ) of amplicon cluster in plastic tube was calculated to be at the level of  $10^{-6} \text{ mm}^2 \text{ s}^{-1}$  at room temperature. Therefore, the diffusion effect on amplicon cluster during rapid PCR amplification (within 5 min) could be ignored.

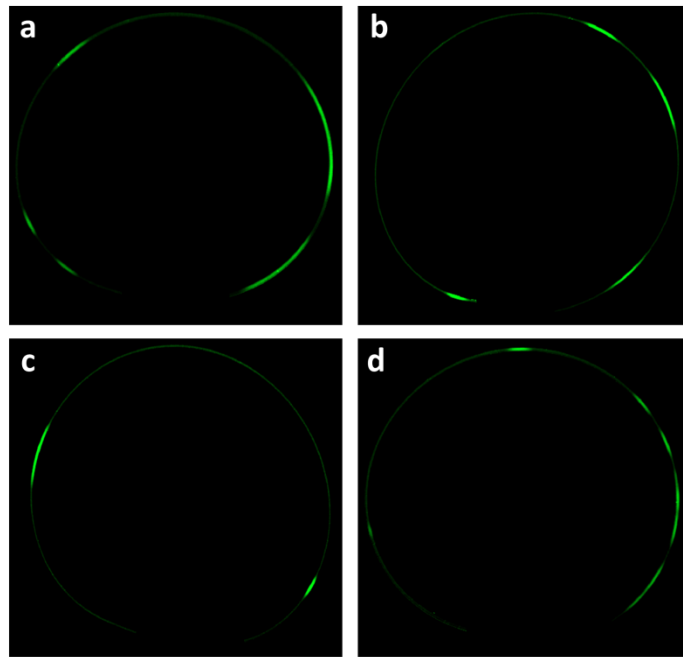


**Figure S13** Four excluded samples that containing amplicon cluster segments not qualified.

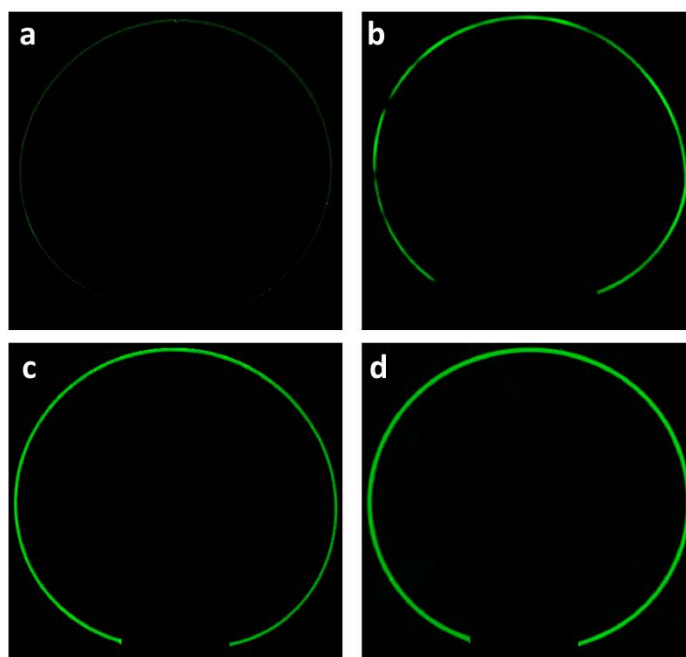


**Figure S14** Images of samples with different amount of DNA targets after rapid PCR amplification. No template control was shown as (a). Sample with  $10^2$ -fold diluted, 10-fold diluted and initial concentration of soybean genetic DNA was shown in (b), (c), (d), respectively.

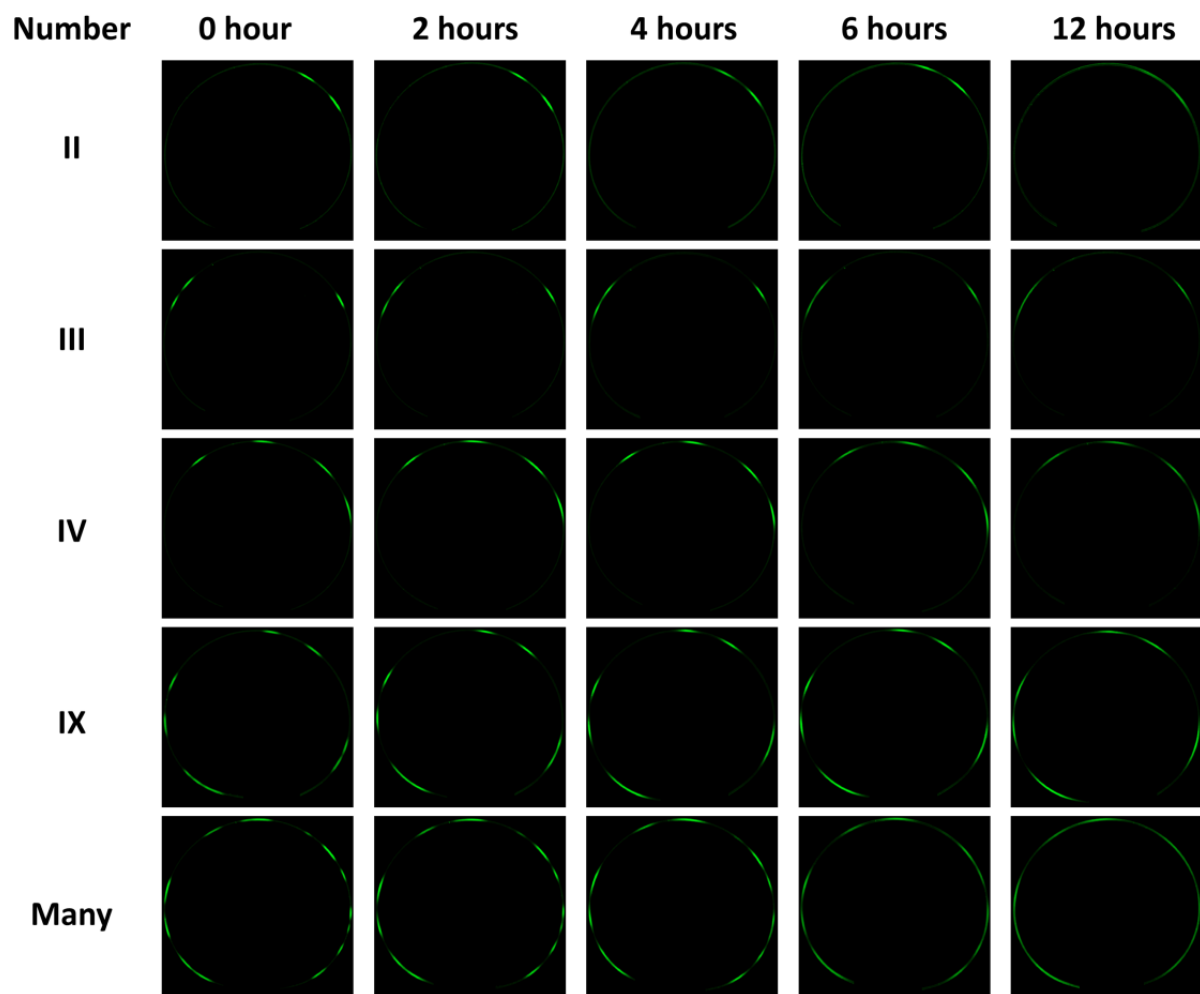


**Figure S15** Study of amplicon cluster diffusion process under room temperature. Initial amplicon numbers in each line were 2 (II), 3 (III), 4 (IV), 9 (IX) and many, respectively. Each sample was imaged under UV light after standing at room temperature for 0, 2, 4, 6 and 12 hours.

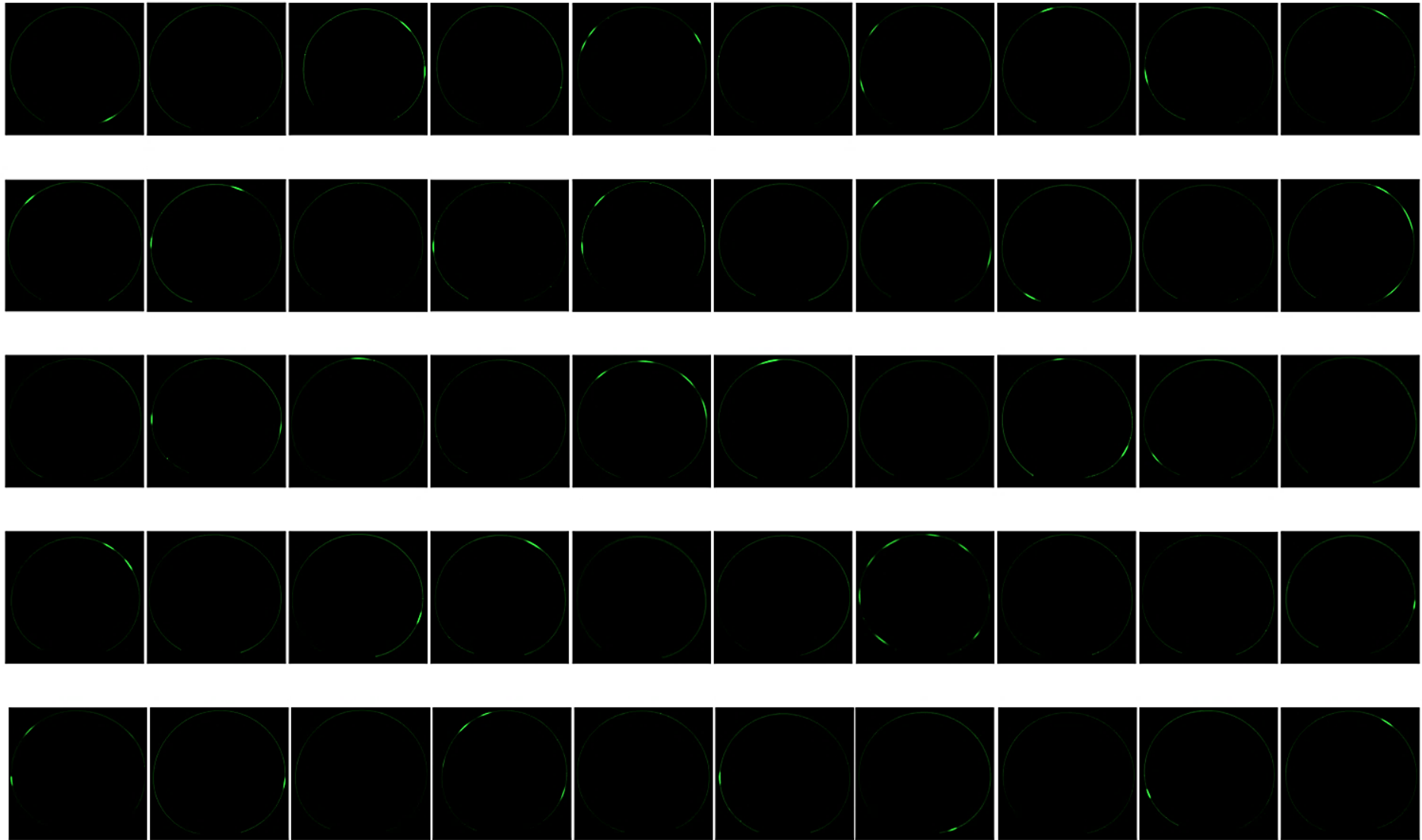


**Figure S16** Images of amplicon clusters for 50 samples.

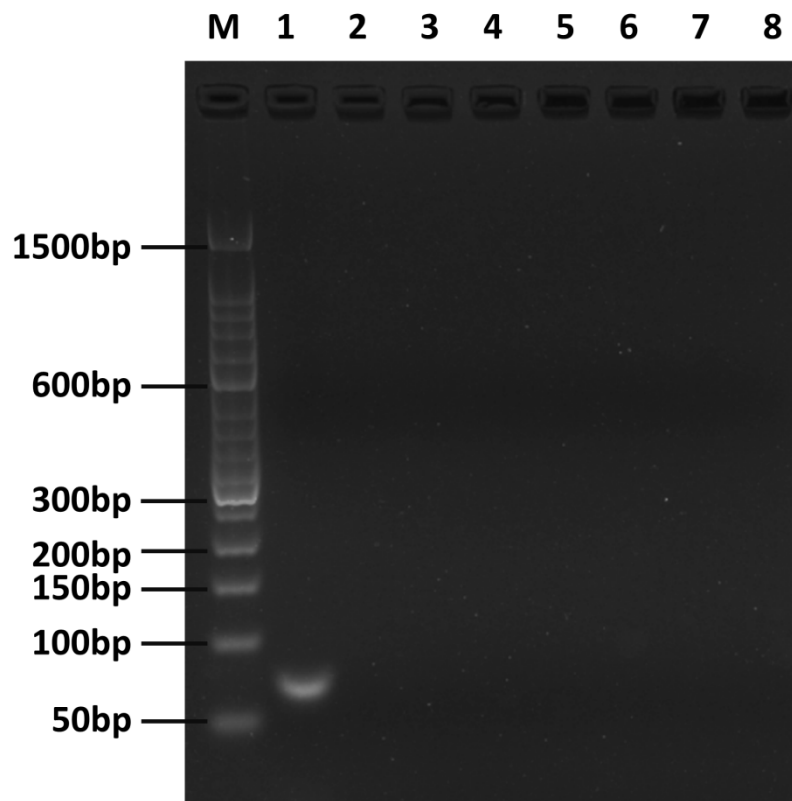


**Figure S17** Detection specificity of rapid PCR amplification in flexible thin tube for *CaMV35S* gene determination. From lane 1-8, the tested samples were LL601 rice, DP 305423 soybean, DP 356043 soybean, non-transgenic soybean, maize, rice, oilseed rape and beet, respectively. M, 50 bp DNA ladder.

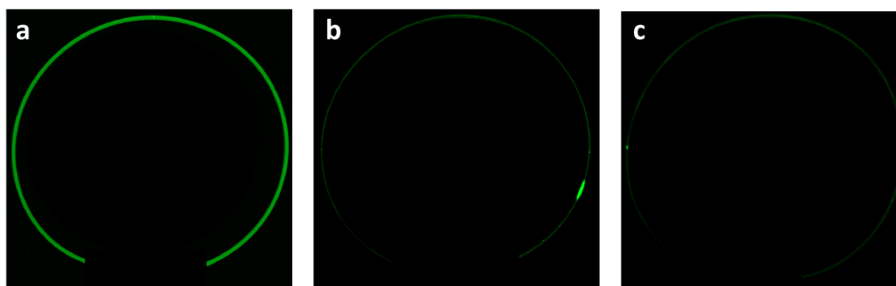


**Figure S18** The image result of rapid PCR amplification in flexible thin tube for *CaMV35S* gene detection with undiluted LL601rice DNA template (a) ,  $10^5$ -fold diluted template whose concentration was at single DNA molecule level (b), with no template added as negative control (c).

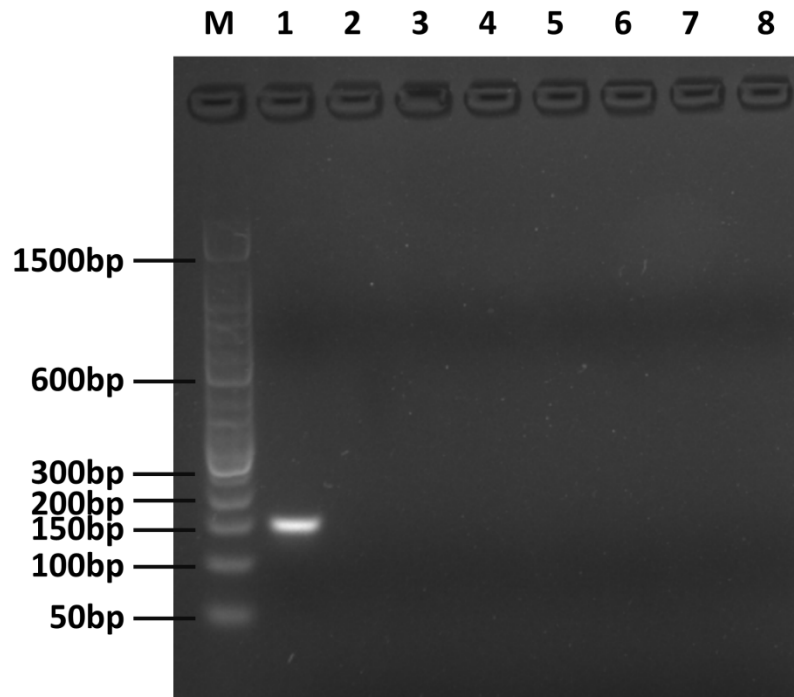


**Figure S19** Detection specificity of rapid PCR amplification in flexible thin tube for *tlh* gene determination. From lane 1-8, the tested samples were *Vibrio parahaemolyticus* (ATCC33847), *Escherichia coli* O157:H7 (ATCC43889) *Saccharomyces cerevisiae* (CICC 1374), *Listeria monocytogenes* (ATCC 19151), *Escherichia coli* (ATCC25922), *Salmonella typhimurium* (ATCC14028), *Escherichia coli* K12 (ATCC29425) and *Bacillus subtilis* (ATCC6633), respectively. M, 50 bp DNA ladder.

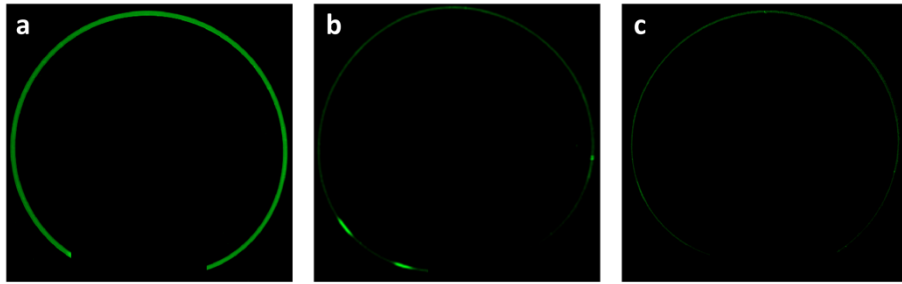
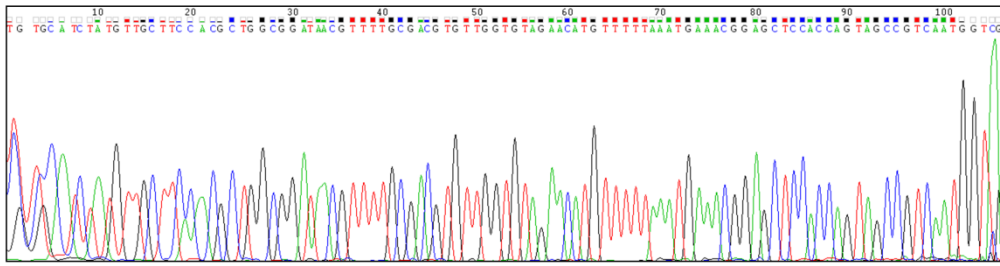


**Figure S20** The image result of rapid PCR amplification in flexible thin tube for *ilh* gene detection with undiluted *Vibrio parahaemolyticus* (ATCC33847) template (a) ,  $10^4$ -fold diluted template whose concentration was at single DNA molecule level (b), with no template added as negative control (c).



Vibrio parahaemolyticus strain MAVP-R plasmid p2, complete sequence

Sequence ID: [CP022555.1](#) Length: 1807442 Number of Matches: 1

Range 1: 1187707 to 1187843 [GenBank](#) [Graphics](#)

▼ Next Match ▲ Previous Match

Score	Expect	Identities	Gaps	Strand
248 bits(134)	3e-62	136/137(99%)	0/137(0%)	Plus/Plus
Query 1	ATTGACGGCTACTGGTGGAGCTCCGTTTCATTTAAAAACATGTTCTACACCAACACGTCG	60		
Sbjct 1187707	ATTGACGGCTACTGGTGGAGCTCCGTTTCATTTAAAAACATGTTCTACACCAACACGTCG	1187766		
Query 61	CAAAACGTTATCCGCCAGCGTTGTGAAGCAACATTAGATTTGGCGAACGAGAACGCAGAC	120		
Sbjct 1187767	CAAAACGTTATCCGTCAGCGTTGTGAAGCAACATTAGATTTGGCGAACGAGAACGCAGAC	1187826		
Query 121	ATTACGTTCTTCGCCGC	137		
Sbjct 1187827	ATTACGTTCTTCGCCGC	1187843		

**Figure S21** Sequencing and blast results of rapid PCR amplification for *tlh* gene detection with  $10^4$ -fold diluted *Vibrio parahaemolyticus* (ATCC33847) DNA as template.

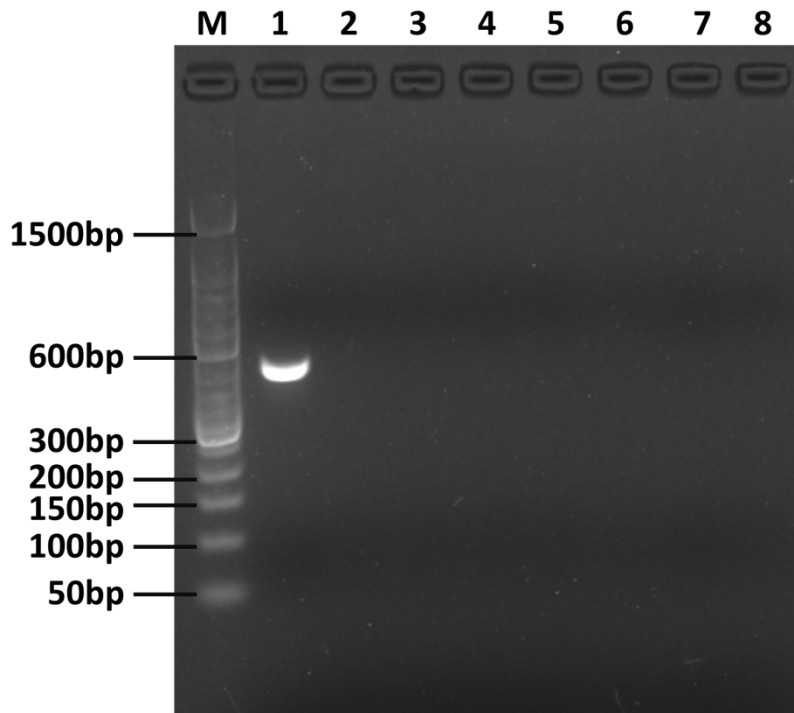


**Figure S22** Detection specificity of rapid PCR amplification in flexible thin tube for *IHHNV* gene determination. From lane 1-8, the tested samples were *Infectious hypodermal and hematopoietic necrosis virus*, *Vibrio parahaemolyticus* (ATCC33847), *Escherichia coli* O157:H7 (ATCC43889) *Saccharomyces cerevisiae* (CICC 1374), *Listeria monocytogenes* (ATCC 19151), *Escherichia coli* (ATCC25922), *Salmonella typhimurium* (ATCC 14028) and *Escherichia coli* K12 (ATCC29425), respectively. M, 50 bp DNA ladder. For *IHHNV* gene detection, 10 s per cycle was performed for rapid PCR amplification.

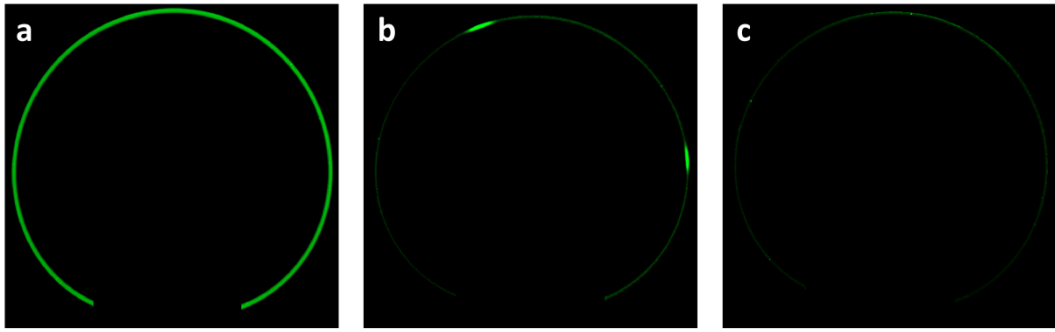
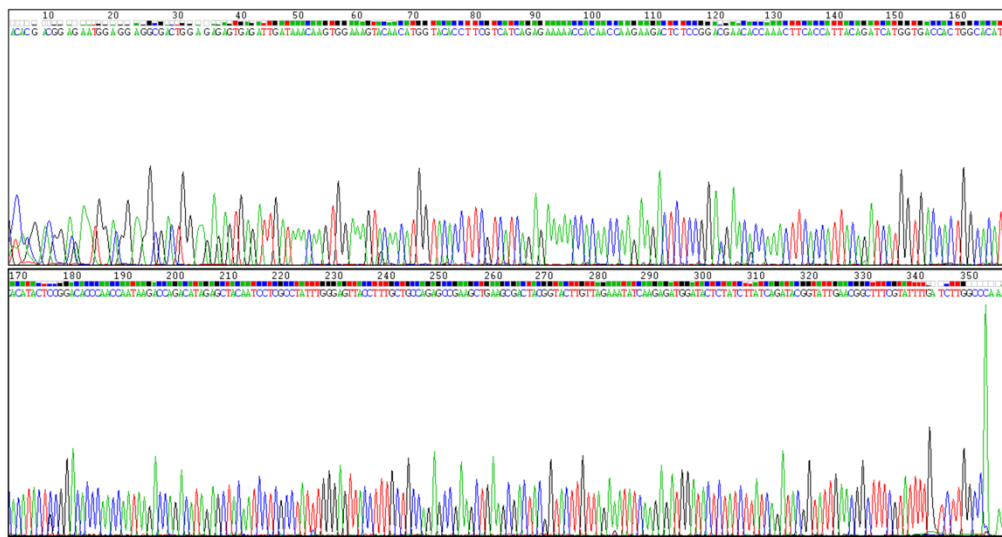


**Figure S23** The image result of rapid PCR amplification in flexible thin tube for *IHHNV* gene detection with undiluted *infectious hypodermal and hematopoietic necrosis virus* template (a) ,  $10^4$ -fold diluted template whose concentration was at single DNA molecule level (b), with no template added as negative control (c).



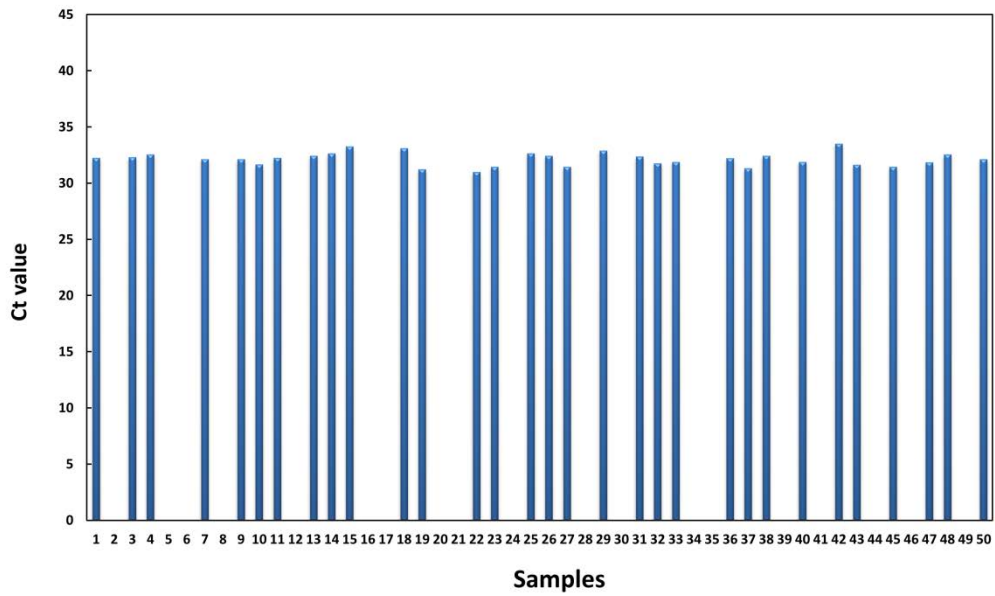
Infectious hypodermal and hematopoietic necrosis virus isolate IHNV2 nonstructural protein 2 (NS2) gene, partial cds  
 Sequence ID: [KF805629.1](#) Length: 389 Number of Matches: 1

Range 1: 15 to 386 [GenBank](#) [Graphics](#) ▼ Next Match ▲ Previous Match

Score	Expect	Identities	Gaps	Strand
673 bits(364)	0.0	369/372(99%)	0/372(0%)	Plus/Plus
Query 1	ACTTTATTGAAGGGACTCCCAACGGACCGGAACGAAATGGACCGAAGGCGACTGGAACACA			60
Sbjct 15	ACTTTATTGAAGGGACTCCCAACGGACCGGAACGAAATGGACCGAAGGCGACTGGAACACA			74
Query 61	CTGAGATTGATAAAACAAGTGGAAACTACAACATGCTACAACCTTCCTCATCAGAGAAAAAC			120
Sbjct 75	CTGAGATTGATAAAACAAGTGGAAACTACAACATGCTACAACCTTCCTCATCAGAGAAAAAC			134
Query 121	CACAACCAAGAAAGACTCTCCGGANGAACACAAAACCTCACCATTACAGATCATCGTGACC			180
Sbjct 135	CACAACCAAGAAAGACTCTCCGGANGAACACAAAACCTCACCATTACAGATCATCGTGACC			194
Query 181	ACTGGCACATCACATACTCCGGACACCAACCAATAAGACCAGACATAGAGCTACAATCC			240
Sbjct 195	ACTGGCACATCACATACTCCGGACACCAACCAATAAGACCAGACATAGAGCTACAATCC			254
Query 241	TGCOCTATTTGGGACTTAOCTTTGCTGCCAGAGCGGAAGCTGAAGCGACTACGGTACTTG			300
Sbjct 255	TGCOCTATTTGGGACTTAOCTTTGCTGCCAGAGCGGAAGCTGAAGCGACTACGGTACTTG			314
Query 301	TTAGAAATATCAAGAGATGGATACTCTATCTTATCAGATACGGTATTGAAACGGCTTTTCT			360
Sbjct 315	TTAGAAATATCAAGAGATGGATACTCTATCTTATCAGATACGGTATTGAAACGGCTTTTCT			374
Query 361	ATTTTCATCTTG			372
Sbjct 375	ATTTTCATCTTG			386

**Figure S24** Sequencing and blast results of rapid PCR amplification for *IHNV* gene detection with  $10^4$ -fold diluted *infectious hypodermal and hematopoietic necrosis virus* DNA as template.

(a)



(b)

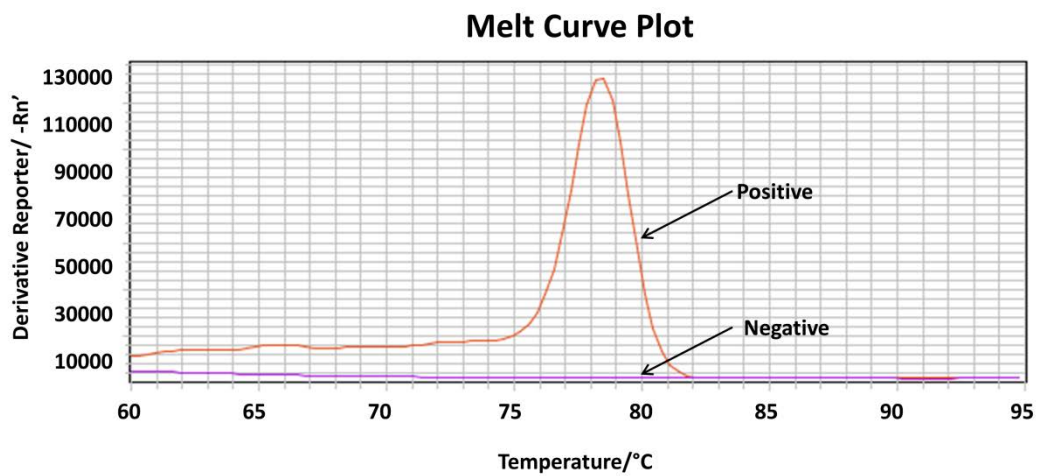


**Figure S25** Traditional PCR detection results of 50 samples for *T-nos* gene detection with template concentration at single molecule level. a) The threshold cycle (Ct) value of 50 tested samples. b) The melt curves of one positive sample (red) and one negative sample (pink).

## References

- 1 G. Wong, I. Wong, K. Chan, Y. Hsieh and S. Wong, *Plos One*, 2015, **10**, e0131701.
- 2 R. Wang, F. Zhang, L. Wang, W. Qian, C. Qian, J. Wu and Y. Ying, *Anal. Chem.* 2017, **89**, 4413-4418.
- 3 K. Arumuganathan and E. D. Earle, *Plant Mol. Biol. Rep.* 1991, **9**, 208-218.
- 4 B. Weidenfeller, M. Höfer and F. R. Schilling, *Compos. Part A-Appl. S.* 2004, **35**, 423-429.
- 5 J. M. Trauba and C. T. Wittwer, *J. Biomed. Sci. Eng.* 2017, **10**, 219-231.